Pharmaceutical Research, Vol. 25, No. 3, March 2008 (© 2007)
DOI: 10.1007/s11095-007-9418-x

Research Paper

Comparative Physicochemical Characterization of Phospholipids Complex of Puerarin Formulated by Conventional and Supercritical Methods

Ying Li,[1,2,3] Da-Jian Yang,[3,5] Shi-Lin Chen,[3,4] Si-Bao Chen,[3,4] and Albert Sun-Chi Chan[3]

Received March 22, 2007; accepted July 20, 2007; published online September 8, 2007

Purpose. The aim of this work was to compare the physicochemical characteristics of the phospholipids complex of puerarin (Pur) prepared by traditional methods (solvent evaporation, freeze-drying and micronization) and a supercritical fluid (SCF) technology. The physicochemical properties of the pure drug and the corresponding products prepared by two different SCF methods were also compared.
Methods. Solid-state characterization of particles included differential scanning calorimetry (DSC), X-ray powder diffraction (XRPD), solubility, dissolution rate and scanning electron microscopy (SEM) examinations. Besides puerarin phospholipids complex (PPC) by four different methods, the solid-state properties of unprocessed, gas antisolvent (GAS) crystallized and solution enhanced dispersion by supercritical fluid (SEDS) precipitated puerarin samples were also compared. Crystallinity was assessed using DSC and XRPD. Drug-phospholipids interactions were characterized using Fourier transform infrared spectroscopy (FTIR). SEM was used to determine any morphological changes. Pharmaceutical performance was assessed in dissolution rate and solubility tests.
Result. The results of the physical characterization attested a substantial correspondence of the solid state of the drug before and after treatment with GAS technique, whereas a pronounced change in size and morphology of the drug crystals was noticed. The GAS-processed puerarin exhibited a better crystal shape confirmed by DSC, XRPD and IR. Polymorphic change of puerarin during SEDS coupled with the dramatic reduction of the dimensions determined a remarkable enhancement of its solubility and *in vitro* dissolution rate. Phospholipids complex prepared using supercritical fluid technology showed similar properties of physical state, thermal stability and molecular interaction with phospholipids (PC) to those of corresponding systems prepared by other three conventional methods namely solvent evaporation, freeze-drying and micronization as proved by XRPD, DSC, and FTIR. The best dissolution rate was obtained by SEDS-prepared complex, while the highest solubility was obtained for solvent evaporation method.
Conclusion. Supercritical fluid technology for the preparation of puerarin and its phospholipids complex has been proven to have significant advantages over the solvent evaporation technique and other conventional methods.

KEY WORDS: microparticles; phospholipids complex; physicochemical characterization; puerarin; supercritical fluids.

[1] Shanghai Jiao Tong University, Shanghai, PR China.
[2] Shenzhen Virtual University Park Postdoc Station, Shenzhen, PR China.
[3] State Key Laboratory of Chinese Medicine and Molecular Pharmacology, 6/F, Block R2-A, Southern Area of the Shenzhen Hi-Tech Park Nanshan District, Shenzhen, PR China.
[4] Institute of Medicinal Plant Development, Chinese Academy of Medical College, Beijing, PR China.
[5] To whom correspondence should be addressed. (e-mail: bcyangdj@inet.polyu.edu.hk)

NOTATION: Co, drug concentration in medium; Cs, saturated concentration in the diffused layer; D, diffusion coefficient; DSC, differential scanning calorimetry; EC, ethyl cellulose; FD-PPC, puerarin phospholipids complex prepared by freeze-drying method; FTIR, Fourier transform infrared spectroscopy; GAS, gas antisolvent; GAS-PC, phospholipids prepared by GAS method; GAS-Pur, puerarin prepared by GAS method; H, diffusion layer thickness; MPPC, puerarin phospholipids complex prepared by micronization method; PC, phospholipids; PEG, poly ethylene glycol; PLA, poly lactic acid; PM, physical mixture of puerarin and phospholipids; PPC, puerarin phospholipids complex; Pur, puerarin; PVP, polyvinyl pyrrolidone; RESS, rapid expansion of supercritical solution; S, surface area; SAS, supercritical antisolvent precipitation; SC-CO_2, supercritical CO_2; SCF, supercritical fluid; SEDS, solution enhanced dispersion by supercritical fluid; SEM, scanning electron microscopy; SEDS-PC, phospholipids prepared by SEDS method; SEDS-PPC, puerarin phospholipids complex prepared by SEDS method; SEDS-Pur, puerarin prepared by SEDS method; SE-PPC, puerarin phospholipids complex prepared by solvent evaporation method; UV, ultra violet; V, medium volume; XRPD, X-ray powder diffraction.

INTRODUCTION

With the application of modern isolation technology and high throughput biological screen capability, more and more natural compounds with biological activity are being isolated and identified. However, many of these compounds with potent activity *in vitro* fail to generate good activity *in vivo* owing to their poor water-solubility, poor permeability and/or poor stability (1). Puerarin was such a drug.

Puerarin, the most abundant isoflavone C-glucoside isolated from *Pueraria lobata* (wild.) Ohwi, has been shown to have beneficial effects on cardiovascular, neurological and hyperglycemic disorders. Pur is clinically used in the treatment of diseases such as angina, myocardial infarction, arrhythmia, hyper-viscous blood, hypertension, cerebral infarction, diabetes, β-hypersensitivity, hypersensitivity, and retinal artery obstruction, etc. However, the strong hydrophilicity and poor liposolubility of Pur limit its absorption *in vivo* (2–6). Solubilizer is often added to the injection formulation used clinically to increase its solubility. Previous pharmacokinetic studies have indicated that Pur is available in intravenous and oral routes, and is rapidly absorbed following oral administration with drug concentrations detectable in the plasma within 30 min. However, the amount absorbed is very small (7–9). Ruan *et al*. determined that puerarin had medium permeability with the apparent permeability of $2.35\pm0.27\times10^{-6}$ cm/s (1). Prasain *et al*. found the persistence of puerarin in blood and urine as the principal metabolic form for the period of 4–72 h after oral administration, suggesting that puerarin was rapidly absorbed from the intestine without metabolism (10). Andrean L. Simons *et al*. also approved that puerarin was resistant to degradation by the gut microflora (11). The study on the absorption kinetics of puerarin in rat intestines revealed that the absorption of puerarin in rats was a first-order process and the mechanism of absorption was passive diffusion transport (12). What's more, the solubilities of Pur in water, 0.1 mol/l HCl and pH 6.8 PBS are 2.87, 3.84 and 3.87 mg/ml separately. The oral dose of Pur in the final dosage form is 400 mg every time, three times each day. So the dose/solubility ratio is about 140 ml. Our previous research has shown the absolute bioavailability of Pur was only about 4.00%. Thus the puerarin should be defined as Class III drug substance according to the Biopharmaceutics Classification System (BCS) Guidance with low permeability and high solubility. By complexing with phospholipids, both the permeability and lipophilicity of puerarin were expected to be improved and ultimately the oral bioavailability could be improved.

Composite particles formation by incorporating active compounds with hydrophilic excipient such as cyclodextrin-type molecule or lipophilic excipient such as phospholipids is one way leading to promising results in terms of bioavailability enhancement (13). Especially the latter, a drug phospholipids complex, defined as integrating one or more natural active components with phospholipids, is a frequently used technique adopted to increase bioavailability and enhance the pharmacological actions of active constituents (14). In comparison with its original state, the drug's lipophilicity can be increased because phospholipids were one of the constituents of the biological membrane, and it helps the combination of drugs with the cell membrane. Thus some physicochemical and biological properties are also enhanced in the complex. The proven successes in promoting the absorption of a variety of natural substances by phospholipids complex formation include silybin (15), dilichol (16), saponins from *Centella asiatica* (17), herba epimedii total flavonoids (18), baicalin (19), diclofenac (20) and piroxicam (21).

In our previous work we improved the oral absorption and tissue distribution properties of puerarin by the preparation of its phospholipids complex using conventional solvent evaporation technique (22,23). But the conventional formulation methods employed for the preparation of drug-phospholipids complex, most frequently solvent evaporation, are always time-consuming and involve multi-stage processing. In addition, the dissolution of PPC was not improved ideally. Parameters related to solid morphology including the particle size, the crystal habit and crystal pattern influence the dissolution rate of a compound and thus can significantly affect their bioavailability (24). So the SCF process was used to enhance the dissolution of PPC and to simplify the experimental procedures for preparing PPC.

In recent years supercritical antisolvent precipitation (SAS) which is one of the SCF technologies is becoming a promising technique that can be used to produce micronic and submicronic particles with controlled size and size distribution. The process is characterized by very mild conditions of temperature, and smaller particles can be obtained depending on the drug and process conditions when compared to the common industrial comminution techniques like jet milling, liquid antisolvent precipitation and crystallization (25,26). Particle size is particularly related to the dissolution of drugs and thus can significantly affect their bioavailability. According to Noyes-Whitney equation: $dC/dt=DS(Cs–Co)/Vh$, where D is the diffusion coefficient, S is the surface area, Cs is saturated concentration in the diffused layer and Co is the drug concentration in medium, the dissolution rate was proportional to D, S, (Cs–Co) and inverse proportional to the diffusion layer thickness of h and medium volume of V. The smaller the particles are, the bigger the S. Thus the dissolution of the drug or composite formulation could be increased. So here the SAS process was intended to be applied to increase the dissolution of PPC. Compared with another kind of SCF method, namely the rapid expansion of supercritical solution (RESS), the SAS is mostly used for recrystallization of powders, or formation of pharmaceutical composites, because of the most important limitation of RESS development being the excessively low solubility of substances in supercritical fluids (27). It has now been clearly established that supercritical fluids especially supercritical carbon dioxide are particle or pharmaceutical formulations formation media of great interest because they offer the possibility of processing materials as diverse as polymers, proteins, and inorganics, with minimized quantity of solvent or even in solvent-free conditions (28). Several research groups have presented their techniques or methods for using supercritical fluids in particle preparation, microencapsulation, surface coating of an active substance particle with a polymer or co-crystallization, co-precipitation with excipients such as polyvinyl pyrrolidone (PVP), poly ethylene glycol (PEG), ethyl cellulose (EC), poly lactic acid

(PLA), Gelucire and other polymers, or host molecules like cyclodextrins (29–40). In addition to micronization, the pharmaceutical application of the SCF process enables to modify the solid-state properties of drug particles. The SAS process including GAS and SEDS can vary the experimental conditions for nucleation and crystal growth steps in a wide range. Hence, particles having different internal crystalline structures and external characteristics can be precipitated (41). According to previous literatures, only two references about preparing phospholipids particles with SCF process by E. Badens research group (28,42) have been republished. But only the neat phospholipids microparticles were prepared without drug loading, and the methods employed for preparing phospholipids were RESS and ASES. In our research, the neat puerarin and the neat phospholipids micriparticles are prepared by other two different SCF methods, meaning GAS and SEDS and their physicochemical characteristics were compared for the first time. Further, no pharmaceutical solid phospholipids complex has previously been reported to be produced using any supercritical fluid processing, and process employed for the preparation of complex may influence the properties of the resulting product. The PPC by SCF method was expected to have better physicochemical characterization.

Two different SCF technologies, GAS and SEDS, belonging to SAS process, were used in this research. In the GAS process, mass transfer typically occurs by the mechanism of convection and molecular diffusion, leading to relatively small supersaturation for many solutes. Although, theoretically, very slow expansion in the GAS process should produce a homogeneous supersaturated solution, such expansion is very difficult to control. In addition, it is impossible to achieve high supersaturation levels in the GAS because of the faster process of nucleation. In the SEDS process, premixing is created between a fresh liquid solution and SC–CO_2, which produces high supersaturation and predominantly occurs within the nozzle mixing chamber (43). This process features a highly turbulent flow of solvent and CO_2, leading to a very fast mixing or dispersion. Thus, mass transfer is not limited by molecular diffusion or convective phenomena. By using this technique, it is possible to control the size, shape and morphology of the material of interest (44). So in our previous research, precipitation of puerarin or phospholipids by GAS method and their complex by SEDS could be obtained successfully for the first time by the optimization of the experimental conditions (to be published), yet the attempts for preparing PPC with GAS failed.

In this work, we aimed to compare the characteristics of these systems with corresponding systems prepared by different conventional methods. Meanwhile the unprocessed drug and puerarin prepared by two different SCF methods were also compared concerning the physicochemical properties. Puerarin was used as the model drug and absolute ethanol as the solvent. Since very few comparisons of the *in vitro* performance of conventional and supercritical-based phospholipids complex are found in literature, attempts have been done in this study to compare the conventional and SCF methods and their effect on the crystal habit, rate and extent of dissolution of PPC, and pharmaceutical performance by DSC, XRPD, FTIR, solubility and dissolution rate for the first time.

MATERIALS AND METHODS

Chemicals

Absolute ethanol (Analytical grade, purity 99.7%) was bought from Guangzhou Chemical Reagent 2 Factory (Guangzhou, China). Puerarin was obtained from Beijing Union Pharmaceutical Factory (Beijing, China). Soya phospholipids PC70 was purchased from Degussa Texturant system Deutschland GmbH&Co. KG (Ausschlager Elbdeich, Hamberg); Liquid CO_2 (Instrument grade, purity 99.5%) was purchased from Zhonghong Industrial Gas (Shenzhen) Co. Ltd. (Shenzhen, China).

Micronization of Pur, PC or PPC by SEDS (SEDS–Pur, SEDS–PC and SEDS–PPC)

The CO_2 passed through a heat exchanger to ensure that it was supercritical before entering the nozzle with the diameter of 0.1 mm, which consisted of two concentric tubes and a small premixing chamber. The schematic diagram of the nozzle was shown in Fig. 1. The mixing solution of puerarin and phospholipids or the single component solution and the supercritical antisolvent were continuously added by two pumps, one for delivering liquid CO_2, and the other for drug solution. Both of them were controlled by Isco Series D pump power controller (Teledyne Isco, Inc., Lincoln, NE) to the precipitation vessel (Thar Designs Inc., Pittsburgh, PA) in co-current mode through the nozzle. The temperature of the vessel was maintained in an Athena heater (Model 2000-B, Athena Controls, Inc., Plymouth Meeting, PA). The high velocity of the supercritical CO_2 (SC–CO_2) stream thoroughly mixed and dispersed the solvent stream and extracted solvent, leaving dry powder in the vessel. The particles formed were collected at the end of the experimental runs. The SC–CO_2 leaved the high-pressure vessel and flowed to the backpressure regulator, which controlled the pressure discharge in the system. The contents of the residual organic solvents within the microparticles were reduced by a washing step for 90 min or more to remove any residual solvent to avoid the re-condensation of the liquid inside the chamber. The vessel was then slowly depressurized for 60 min and the powder removed. The conditions optimized for preparing puerarin or its complex were as bellows: temperature 35°C pressure 10 mpa, flow rate of CO_2 45 ml/min, flow rate ratio

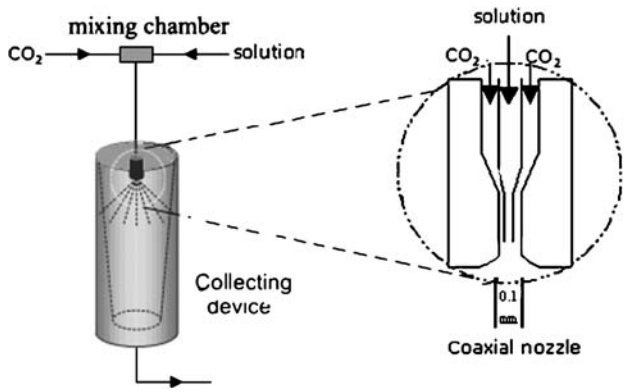

Fig. 1. Schematic diagram of the nozzle in SEDS apparatus.

of drug to CO_2 solution 1%, the mass ratio of drug to phospholipids used for preparing PPC in all methods retaining 1:1.2, and concentration of puerarin 100 mg/ml. Handling and storage conditions for SCF products were identical to the conventional processed PPC. The yields of SEDS–Pur, SEDS–PC and SEDS–PPC were 95.1, 64.0 and 93.3%. The theoretical value of SEDS–PPC drug payload was 45.5%, and the experimentally quantified value was 44.5%.

Preparation of Puerarin or Phospholipids by GAS Precipitation (GAS-Pur and GAS-PC)

The equipment for GAS is almost the same with SEDS except that the pump controller in charge of delivering drug solution was not turned on. The drug solution was not imported into the precipitation vessel by this pump, but was poured into the vessel before the experiment started. In the batch GAS step configuration, the precipitation unit attached to Isco syringe pump was initially loaded with 100 ml of puerarin or 10 ml of phospholipids solution. Then CO_2 was added until the final pressure was reached. The rate of CO_2 addition is 107 ml/min. The volume of the precipitation vessel was 250 ml. The vessel was filled with SC–CO_2 at the desired pressure (10 mpa), temperature (38°C) and left for 3 h without any agitation. A pure constant carbon dioxide flow rate of 25 ml/min was then maintained in order to completely remove the residual solvent. After this washing step which lasted for approximately 90 min, the autoclave was depressurized for 30 min at the experimental temperature. At the end of experiment, solid product was scraped out with a spatula from the filter located at the bottom of the vessel and subjected to handling and storage conditions identical to the unprocessed materials.

Preparation of Puerarin Phospholipids Complex by Conventional Methods

PPC prepared by solvent evaporation (SE–PPC): Drug and phospholipids with mass ratio of 1:1.2 were dissolved in 100 ml of absolute ethanol in a round bottom flask under stirring at the temperature of 30°C. The concentrations of Pur and PC were 100 and 120 mg/ml. The solvent was then removed under reduced pressure in a rotary evaporator (4001 Laborota, Heidolph Instruments GmbH&Co., Schwabach, Germany) at 40°C and 60 rpm. The resultant solid was collected and desiccated in the vacuum ovens at 50°C, then pulverized and finally passed through a 180-μm sieve, and then stored in a desiccator at room temperature.

PPC prepared by freeze-drying (FD–PPC): Drug and phospholipids with mass ratio of 1:1.2 were dissolved in 100 ml of absolute ethanol in a round bottom flask under magnetically stirring at the temperature of 30°C. After half hour, the solution was deep-frozen at −80°C for 24 h in the Heto Ultra Freeze (Model 4410, Heto-Holten A/S, Allerod, Denmark), then lyophilized in a Heto Dry Winner freeze-drier (Model DW8, Heto-Holten A/S, Allerod, Denmark) at −45°C and 0.01 mpa during 48 h. The resulted solid was then collected, pulverized and passed through a 180-μm sieve, and then stored in a desiccator at room temperature.

PPC prepared by micronized puerarin (MPPC): Puerarin used for the preparation of MPPC was firstly micronized to about 500 nm in the BFM-6 Billion micropowder mill (Jinan Billion Powder Tech & Engineering, Shandong, China). Then, micronized puerarin and phospholipids with mass ratio of 1:1.2 were dissolved in 100 ml of absolute ethanol in a round bottom flask under stirring at the temperature of 30°C. Finally, the solvent was removed under reduced pressure in a rotary evaporator.

Preparation of the physical mixture of puerarin and phospholipids (PM): For comparison, a physical mixture of drug and phospholipids was made in the same mass ratio of 1:1.2. The mixture was prepared by mixing Pur and phospholipids thoroughly during 5 min in a mortar until a homogeneous mixture was obtained.

Scanning Electron Microscopy

The shape and surface characteristics of the processed and unprocessed materials were observed with a Jeol JSM-6460LV electron scanning microscope (Japan Electron Optics, Tokyo, Japan). Powder samples were manually dispersed on an aluminum stub with a thin self-adhered carbon film. The samples were coated with a thin layer of gold using an ion sputter under 0.5 mbar argon atmosphere (at room temperature for 90 s, at an accelerating voltage of 20 kv, working distance of 15 mm, and at ×1,000 magnification).

X-ray Powder Diffraction Analysis

The crystalline state of Pur in the different samples was evaluated with X-ray powder diffraction. Diffraction patterns were obtained on a Rigaku D/MAX 1200 diffractometer (Rigaku International, Tokyo, Japan). A graphite monochromator was used. The X-ray generator was operated at 40 kV tube voltages and 40 mA of tube current, using the Ka lines of copper as the radiation source. The scanning angle ranged from 1 to 60° of 2θ in step scan mode (step width 0.4°/min). Pur, phospholipids, their physical mixture and PPC prepared by four different methods were analyzed with X-ray diffractions. The result was shown in Fig. 6.

Differential Scanning Calorimetry

Thermal analysis of Pur, phospholipids, their physical mixture and PPC by four methods were performed in a Netzsch 204 differential scanning calorimeter (Netzsch Instruments, Burlington, Germany). Samples were accurately weighed (1–3 mg) into aluminum pans having pierced lids. Thermograms were obtained at a heating rate of 10°C/min over a temperature range of 25–230°C. The result was shown in Fig. 7.

Infrared Spectroscopic Analysis

FTIR spectra for the various powders were obtained on a 8400 Shimadzu FTIR spectrometer (Shimadzu, Tokyo, Japan) in the transmission mode with the wave number region 500~4,000 cm^{-1}. KBr pellets were prepared by gently mixing 1 mg sample powder with 100 mg KBr. A resolution of 8 cm^{-1} was used and 64 scans were co-added for each spectrum over a frequency range of 500~4,000 cm^{-1}. The result was shown in Fig. 8.

Solubility Studies

The apparent solubility studies for various powders in distilled water were performed by adding an excess amount of the compounds to 20 ml of media in screw capped vials. The vials were allowed to shake at 25±0.5°C for 24 h in water baths. Preliminary experiments had shown that this time period was sufficient to assure saturation. After equilibrium had been attained, the saturated solutions were immediately and rapidly filtered through a 0.45 μm membrane filter and properly diluted with water to prevent crystallization. All the materials used for the filtration was brought to the same temperature as that of the solutions. Each experiment was performed in triplicate and the filtered and diluted solutions were analyzed by Model Lamba 35 Ultra Violet (UV) spectrophotometer (Perkin Elmer Life and Analytical Sciences, MA, USA) from the linear absorbance *versus* concentration relationship.

Dissolution Study

In vitro dissolution studies for each PPC as well as plain puerarin and SEDS-Pur were performed in triplicate in a CP (2005) Dissolution Apparatus II (the paddle method) at 37±1°C and 100 rpm to estimate the improvement in dissolution rate by supercritical fluid process. An accurately weighted amount of the prepared system equivalent to 100 mg of Pur was put into 500 ml artificial gastric solution to maintain sink conditions. A 5.0 ml aliquot was withdrawn with an equal volume of fresh artificial gastric solution supplemented at a fixed time intervals and filtered through a 0.45 μm membrane filter. The concentration of dissolved drug was then measured by UV. In this way the dissolution kinetics were established and compared.

Data analysis

Results are expressed as mean values and standard deviations (±SD) and the significance of the difference observed was analyzed by the Student's *t* test. In all tests, a probability value of $P<0.05$ was considered statistically significant.

RESULTS AND DISCUSSION

The use of different analytical techniques enables us to characterize and compare the physicochemical properties of the prepared solid complex. Microparticles produced by supercritical and conventional methods were characterized by XRPD and DSC. Microparticles morphology was characterized by SEM. IR and solubility, dissolution test were also carried out. What's more, a substance may exist in different forms at solid state. Depending on how the molecules fit together, different polymorphs can be encountered. This can be important in the quality of a given product. In the pharmaceutical field, an active substance may exhibit different activities and shelf life depending on the polymorph (45). So the properties of puerarin and its supercritical fluid products were also compared to investigate the effect of SCF process. Main characteristics of the particles prepared have been listed in Table I.

Table I. Characteristics of the Particles Prepared

System	Method of Preparation	Morphology	Particle Size (μm)	Drug Payload (%)
Unprocessed Pur	–	Composed of variously sized cascading flakes	25.676	–
Unprocessed PC	–	Continuous flat film	4.669	–
SEDS–Pur	Puerarin prepared by SEDS method	Composed of microparticles, large aggregates, no crystal structure	6.467[a]	–
SEDS–PC	Phospholipids prepared by SEDS method	Similar to unprocessed PC	4.916	–
GAS–Pur	Puerarin prepared by GAS method	More ordered appearances with clean surfaces and directionally arranged in prisms	20.395	–
GAS–PC	Phospholipids prepared by GAS method	Similar to unprocessed PC	5.286	–
SEDS–PPC	Puerarin phospholipids complex prepared by SEDS method	Aggregated particles	5.927[b]	44.5
SE–PPC	Puerarin phospholipids complex prepared by solvent evaporation method	Nubby granules wrapped with phospholipids—likely compacted viscous plates	6.323	45.5
FD–PPC	Puerarin phospholipids complex prepared by freeze-drying method	Agglomerated in larger blocks formed by fused plates together	4.907	43.7
MPPC	Puerarin phospholipids complex prepared by micronization method	Nubby granules wrapped with phospholipids—likely compacted viscous plates	6.019	44.9

[a] actually comprised by small near-spherical particles with the size of smaller that 0.5 μm
[b] actually comprised by small near-spherical particles with the size of only about 1 μm

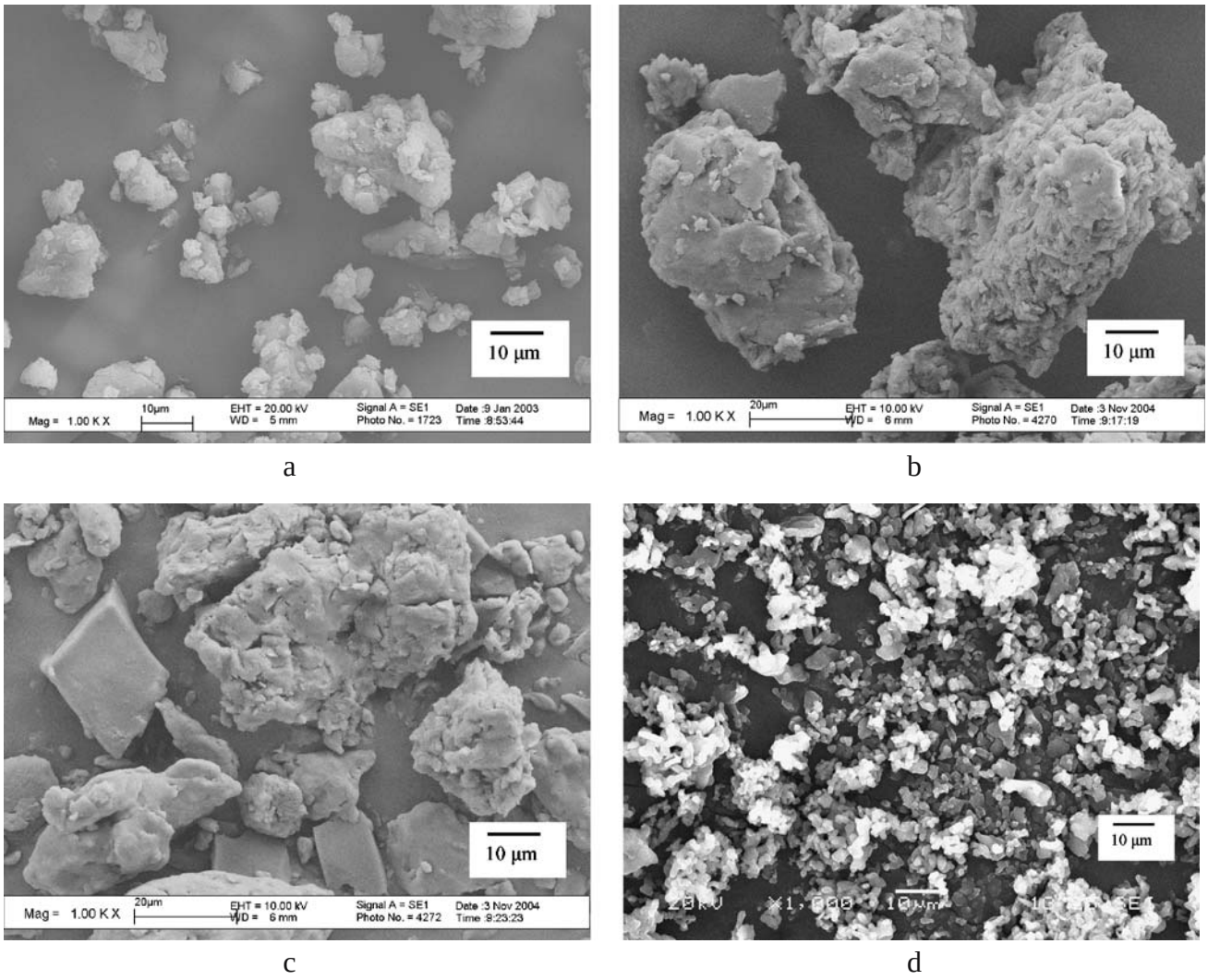

Fig. 2. SEM photographs of PPC particles prepared by different methods: **a** SE_PPC, **b** MPPC, **c** FD-PPC and **d** SEDS-PPC.

Morphology

Figure 2 illustrated that the physical appearances of PPC microparticles by three conventional methods were almost similar except SEDS–PPC. This study revealed no change in powder appearances between MPPC and SE–PPC, exhibiting nubby granules wrapped with phospholipids—likely compacted viscous plates, despite that the micronized Pur was used when preparing MPPC. FD–PPC appeared agglomerated in larger blocks formed by fused plates together. According to the result of particle size, it should be noted that in this study the SEDS–PPC was not sieved or ground which was one of procedures in other three methods, but having the equivalent size with them. And from the SEM, the size of SEDS–PPC was in fact considered to be the size of particle aggregates which were comprised by small near-spherical particles ranging only about 1 μm. Besides the advantage of SEDS method over the particle size reduction, the size distribution was more uniform and the shape more regular. So it is reasonable to predict that SEDS–PPC favors the dissolution process and further oral bioavailability *in vivo*.

Figures 3, 4, 5 showed SEM pictures of puerarin with and without SCF processing and indicated much difference between two kinds of SCF methods and also between Pur prepared by SCF methods and raw material. The unprocessed puerarin was composed of variously sized cascading flakes whilst after processing with GAS, the particles trans-

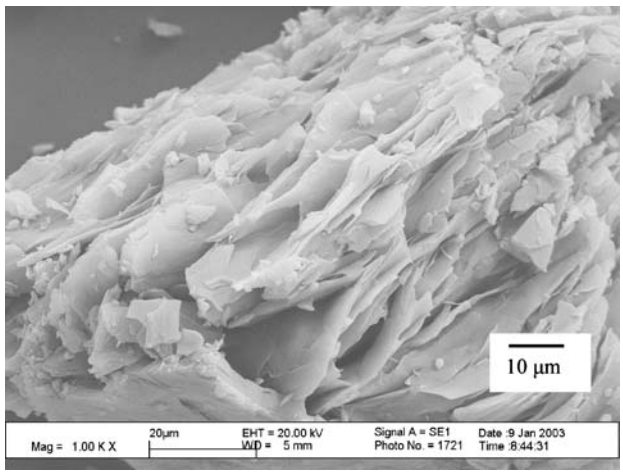

Fig. 3. SEM picture of commercial Pur.

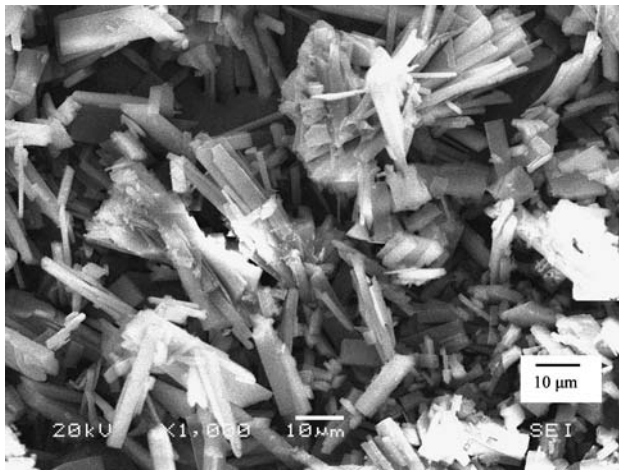

Fig. 4. SEM picture of GAS–Pur.

formed into a totally different crystal form. Overall observation of SEM photomicrographs of the two compounds (Figs. 3 and 4) indicated that the GAS processed crystals exhibit more ordered appearances with clean surfaces and directionally arrangment in prisms. The phenomenon was consistent with the literature (46). This means that the GAS process provides suitable environment for the solid growth of a single crystal, minimizing the conditions for growth-related imperfections and solvent occlusion into the crystal faces. These results showed that the GAS processed crystals may provide the possibility to control and improve the morphology of drug particles and provide another approach for compound recrystalization. On the contrary, SEDS–Pur showed no crystal structure at all. Also in SEM picture the particles were comprised of microparticles whose mostly size was even smaller than 0.5 μm making the nanoparticles preparation possible. Large aggregates were also formed by coalescence of particles due to both the impacts undergone by the particles during the precipitation and the interactions between the solvent and the solute as pointed out by Badens (28). The collected SEDS–Pur sample was a very light, voluminous powder displaying a radically altered gross morphology, which was consistent with the conclusion deduced by Sundeep Sethia *et al.* (30). In their research, the untreated carbamazepine was mainly characterized by well-defined prisms whereas carbamazepine sample processed by SEDS was a very light, voluminous powder. Determination of the specific surface area also confirmed that the specific surface area was doubled by SEDS from 0.50 to 1.08. By forming small particles with higher surface areas would further increase the drug release rate.

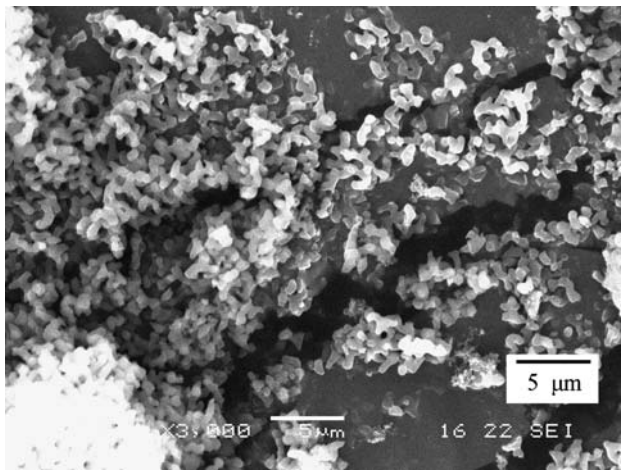

Fig. 5. SEM picture of SEDS–Pur.

XRPD Studies

To check whether the changes in the puerarin crystal morphology correspond to a polymorphic transition and to study the solid state of differently processed PPC, XRPD analysis was conducted. From these patterns, the degree of crystallinity could be evaluated using the relative integrated intensity of reflection peaks in the given range of reflecting angle, 2θ. The value of 2θ means the diffraction angle of X-

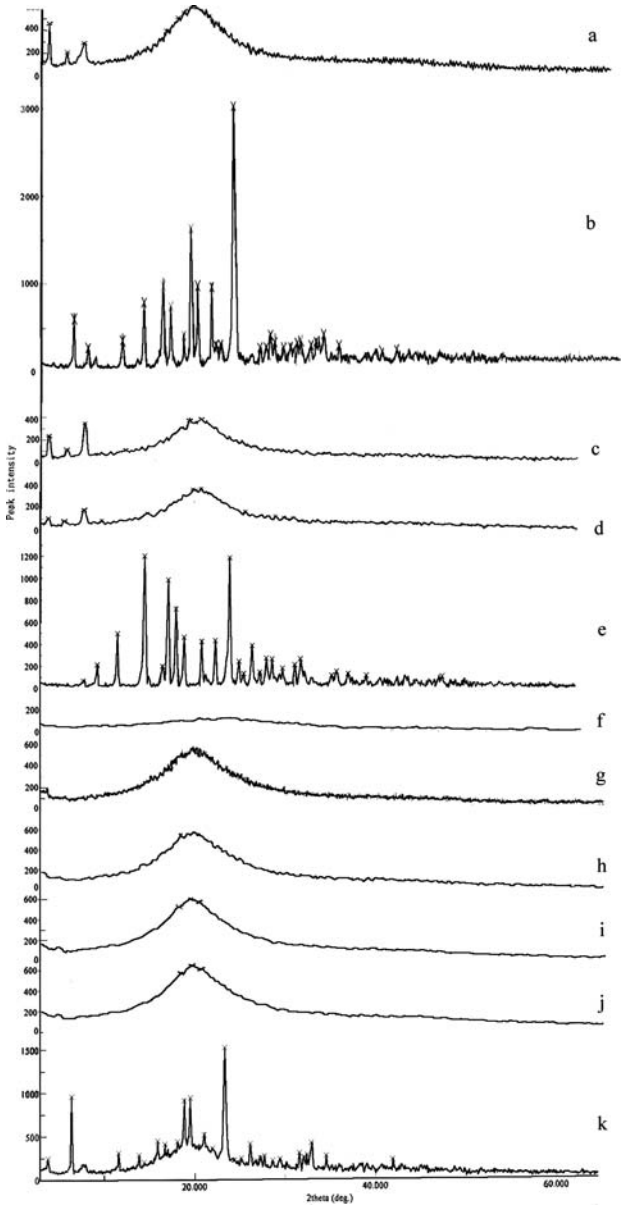

Fig. 6. X-ray diffractograms of **a** unprocessed PC, **b** unprocessed Pur, **c** GAS–PC, **d** SEDS–PC, **e** GAS–Pur, **f** SEDS–Pur, **g** SE–PPC, **h** SEDS–PPC, **i** FD–PPC, **j** MPPC and **k** PM.

Table II. Intensities at Characteristic Diffraction Angles 2θ (°) and *d* values (*Å*) for Unprocessed Pur

2θ	*D* value	Intensity	2θ	*d* value	Intensity
6.460	13.6705	599	27.240	3.2710	382
7.940	11.1254	262	27.700	3.2177	298
11.560	7.6483	349	28.640	3.1142	237
13.860	6.3839	778	29.380	3.0374	232
15.880	5.5761	965	30.080	2.9683	289
16.700	5.3041	729	30.400	2.9378	310
18.080	4.9022	395	31.540	2.8341	262
18.820	4.7111	1615	32.080	2.7877	296
19.560	4.5345	960	32.900	2.7200	377
21.040	4.2188	942	34.500	2.5975	250
21.480	4.1333	275	39.060	2.3041	174
21.940	4.0477	282	40.640	2.181	189
23.320	3.8112	2991			
26.140	3.4061	242			
26.780	3.3261	238			

ray beams, which is shown in the abscissa of Fig. 6. The integrated intensity is given by the area under the curves of the XRPD patterns, and it stands for the characteristics of the specimen (41). The characteristic peaks of Pur, GAS–Pur and their intensities were presented in Tables II and III. Characteristic high-intensity diffraction peaks were detected at 2θ values of 6.460, 13.860, 15.880, 16.700, 18.820, 19.560, 21.040, 23.320 for commercial Pur and 11.280, 14.160, 16.660, 17.480, 18.360, 20.220, 21.660, 23.180 for GAS–Pur, suggesting that puerarin existing in a natural crystalline form and transforming into another form after GAS processing. The difference of XRPD patterns between the unprocessed and processed Pur crystals could be explained by two possible phenomena. They were preferred orientation and polymorphic modification. Preferred orientation was a condition in which the distribution of crystal orientations was nonrandom, and a specific crystalline frame may tend to cluster to a more or less degree about some particular orientations (46). In this study, the XRPD patterns of Pur illustrated the typical behavior of preferred orientation as shown in Fig. 6. These results show that GAS process may control the 'crystal texture' due to the change in crystallinity and preferred orientation. In fact, it was reported that in organic crystals, the rate of crystallization affected preferred orientation, which in turn influenced the physical properties of crystals (46). In our research, the Pur crystal was arranged in directional prisms according to the above reasons. The comparison of Pur patterns showed that Pur was crystalline before processing and amorphous after SEDS process (Fig. 6b and f). This difference can be readily explained by the very fast precipitation process characterizing the SEDS which does not allow the organization of the compound in a crystalline form (25). PC whether processed by SCF method or not being amorphous did not show any peaks besides three small peaks at 2θ and *d* values of 3.880°(22.7530Å), 5.820°(15.1723Å) and 7.660° (11.5314Å), which arose from the fact that it was made up of mixture of glycerine, fatty acid, phospholoric acid, alkamine and cyclol. The treatment of PC with SCF technique did not alter its physical state. Fig. 6g–k reported the XRPD patterns of the binary systems. In the case of PM, XRPD pattern depicted in Fig. 6k was simply the superposition of those of Pur and PC. The sharp peaks indicated the retention of crystalline structure of drug in the physical mixture, but no new peaks could be observed, suggesting no interaction between Pur and the carrier PC. All of the observed XRPD patterns of four different PPC revealed a broad peak similar to PC indicating the puerarin was in amorphous form in PPC prepared by any method. The disappearance of puerarin crystalline diffraction peaks confirmed the formation of phospholipids complex and also was credited to it (47).

DSC Studies

The differential scanning calorimetry is a tool used to measure the temperature and energy variation involved in the phase transitions, which reflects the degree of crystallinity and stability of the solid state of pharmaceutical compounds (46). The peak size and shape of the DSC curves are useful in determining the crystallinity of the drug and the carrier. In recent studies, it has been reported that SCF processing alters the crystallinity of drugs (48). This was confirmed by our preparation of Pur with GAS and SEDS. The DSC curves of pure components and respective drug-carrier (1:1.2, mass ratio) systems prepared by four different methods were shown in Fig. 7. Commercial Pur showed a endotherm at 209.7°C corresponding to its melting peak, also confirming the crystalline nature of the unprocessed drug and a broad endotherm at 94.8°C indicating the loss of water. No peak was detected in the determination range for GAS–Pur. This may be attributable to the drug substance achieving greater purity and higher crystallinity when processed with GAS. The supercritical fluids can extract impurities from the material. So the melting point of Pur increased above 230°C with its higher crystallinity and the corresponding peak could not be detected within the range. To confirm this, later, the DSC of GAS–Pur had been retested and its melting point was determined. The melting point (m.p) determined by Digital Display Binocular Microscope for Melting Point Test (X-5_A, Beijing Focus Instrument Co., LTD, Beijing, China) revealed that the m.p of GAS–Pur was 250–251.5°C. The DSC detection range was also increased to 250°C. In the curve of Fig. 7e, only one sharp and high peak corresponding to the melting peak at 248.6°C was observed at all temper-

Table III. Intensities at Characteristic Diffraction Angles 2θ (°) and *d* values (*Å*) for GAS–Pur

2θ	*D* value	Intensity	2θ	*d* value	Intensity
7.620	11.5918	65	27.060	3.2923	273
9.120	9.6884	213	27.680	3.2200	266
11.280	7.8375	496	28.800	3.0973	180
14.160	6.2493	1,199	30.100	2.9664	212
16.040	5.5208	198	30.700	2.9098	266
16.660	5.3167	984	34.020	2.6330	116
17.480	5.0691	720	34.540	2.5945	153
18.360	4.8281	463	35.760	2.5088	131
20.220	4.3880	424	37.720	2.3828	118
21.660	4.0994	433	45.740	1.9819	109
23.180	3.8339	1,186			
24.160	3.6805	244			
24.660	3.6070	133			
25.560	3.4820	387			
26.360	3.3781	145			

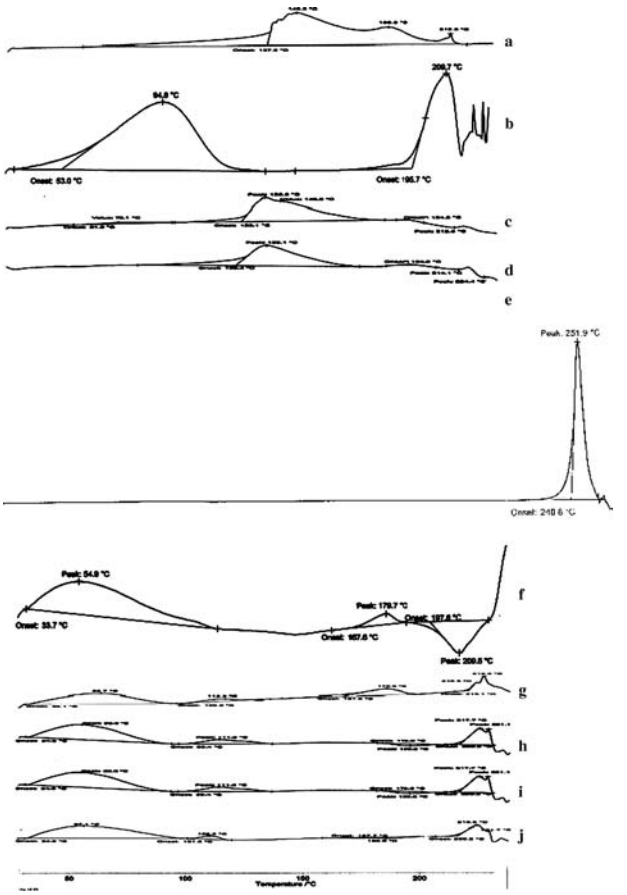

Fig. 7. DSC thermograms of **a** unprocessed PC, **b** unprocessed Pur, **c** GAS–PC, **d** SEDS–PC, **e** GAS–Pur, **f** SEDS–Pur, **g** SE–PPC, **h** SEDS–PPC, **i** FD–PPC and **j** MPPC.

atures investigated. This result indicated that the crystals formed from the GAS recrystallization were stable until the m.p was reached. Compared with the DSC of unprocessed Pur in Fig. 7b, this result also confirmed that the crystals from GAS contain a higher degree of crystallinity deduced from the results of the XRPD pattern study. Scans of SEDS–Pur indicated no presence of melting peak reflecting the crystalline drug converting to amorphous form. But we noticed that the curve of the SEDS–Pur showed two new endothermic transitions at 54.9°C and 179.7°C where the first peak corresponded to the solid/solid transition between two different solid states, and the second peak corresponded to the fusion from solid to liquid state because of the amorphous characteristics. The result was consistent with the previous research of Zhai (49). As a comparison, PC was separately treated with SC–CO_2 and their DSC curves were also depicted in Fig. 7. During scanning of unprocessed PC, a broad endotherm ranging from 149.3~212.5°C was observed. The peak at 149.3°C exhibited a leading shoulder arising from segregation of soy phospholipids components into fractions with different melting points and was very broad. The second peak at 186.8°C was wide and estimated to be the thermal phase change region. The third peak at 212.5°C may be derived from the process of getting the bound water off from phospholipids (50). PC prepared by GAS and SEDS showed similar DSC curves with the descending melting range. Although no change on crystal form existed in PC because of its amorphous nature, the descending melting range was considered to be relevant to its different particle surface between SCF products and raw material. The thermograms of SEDS–PPC, SE–PPC, FD–PPC, and MPPC formulations (Fig. 7g–j) also showed similar four broad endotherms, but no endotherms were observed around the melting point of Pur or PC. The differences between composite and pure components were evident in composites rich in drug, where the drug characteristics controlled the properties of the composite. So this difference may be attributed to the transformation of Pur into an amorphous state, or the formation of a phospholipids complex or a combination of both phenomena since the Pur alone prepared by SEDS was also amorphous (47). Upon SC–CO_2 exposure to PPC, the endothermic peak of PPC in the DSC analysis was not altered compared with other three methods suggesting that the SCF-processing had no effect on the thermal behavior of Pur, an observation consistent with the XRPD results. Since the drug payload of the four kinds of PPC presented in Table I was all more than 40%, the DSC characteristics almost belonged to the drug. The peak at 114.5°C may due to the loss of water. The peak at 219.5°C was also derived from the process of getting the bound water off from phospholipids. Peaks at 63.7 and 179.8°C corresponded to the phase change temperature and the fusion temperature because of the amorphous Pur. Crystallization inhibition was attributed to two effects by phospholipids complex formation: interactions, such as the integration of drug and phospholipids through charge transfer between them; or the entrapment of drug molecules in the phospholipids during solvent evaporation; or a combination of both (51).

IR Studies

FTIR studies were done to detect the possible interaction between Pur and PC in the phospholipids complex leading to amorphous state of Pur and the effect of different methods on the formation mechanisms of PPC (Fig 8). Major absorption bands for various samples were listed in Table IV (52,53). The molecular formula of phospholipids and puerarin are as below in Fig. 9.

Besides hydroxyl stretching band at 3382.9 cm^{-1}, –C–H stretching band of saturated long fatty acid chain at 2923.9 and 2854.5 cm^{-1}, carbonyl stretching band at 1735.8 cm^{-1} in the fatty acid ester, –P=O stretching band at 1238.2 cm^{-1} and –P–O–C stretching band at 1060.8 cm^{-1} in the PC structure, also –OH (ν_{OH}, 3232.5), –C=O($\nu_{C=O}$, 1631.7), –C=C vibration in the benzene-ring($\nu_{C=C}$, 1608.5, 1569.9, 1515.9, 1446.5), –C–O–R(ν_{C-O}, 1010.6) and the –C–C single bond ($\nu_{C-C(benzene)}$, 891.1, 837.0, 798.5) vibration peaks were detected at the same position as that of drug in the IR spectra of PM. The FTIR spectra of physical mixtures seemed to be only a summation of drug and PC spectra. A very broad band was visible at 3382.9 cm^{-1} that was attributed to the presence of water confirming the broad endotherm detected in the DSC experiments. This result suggested that there was no interaction between drug and PC in physical mixture and Pur maintained its crystallinity as observed in thermal analysis and XRPD. On the contrary, in the spectra of the phospholipids complex, shifts, disappearances or attenuation

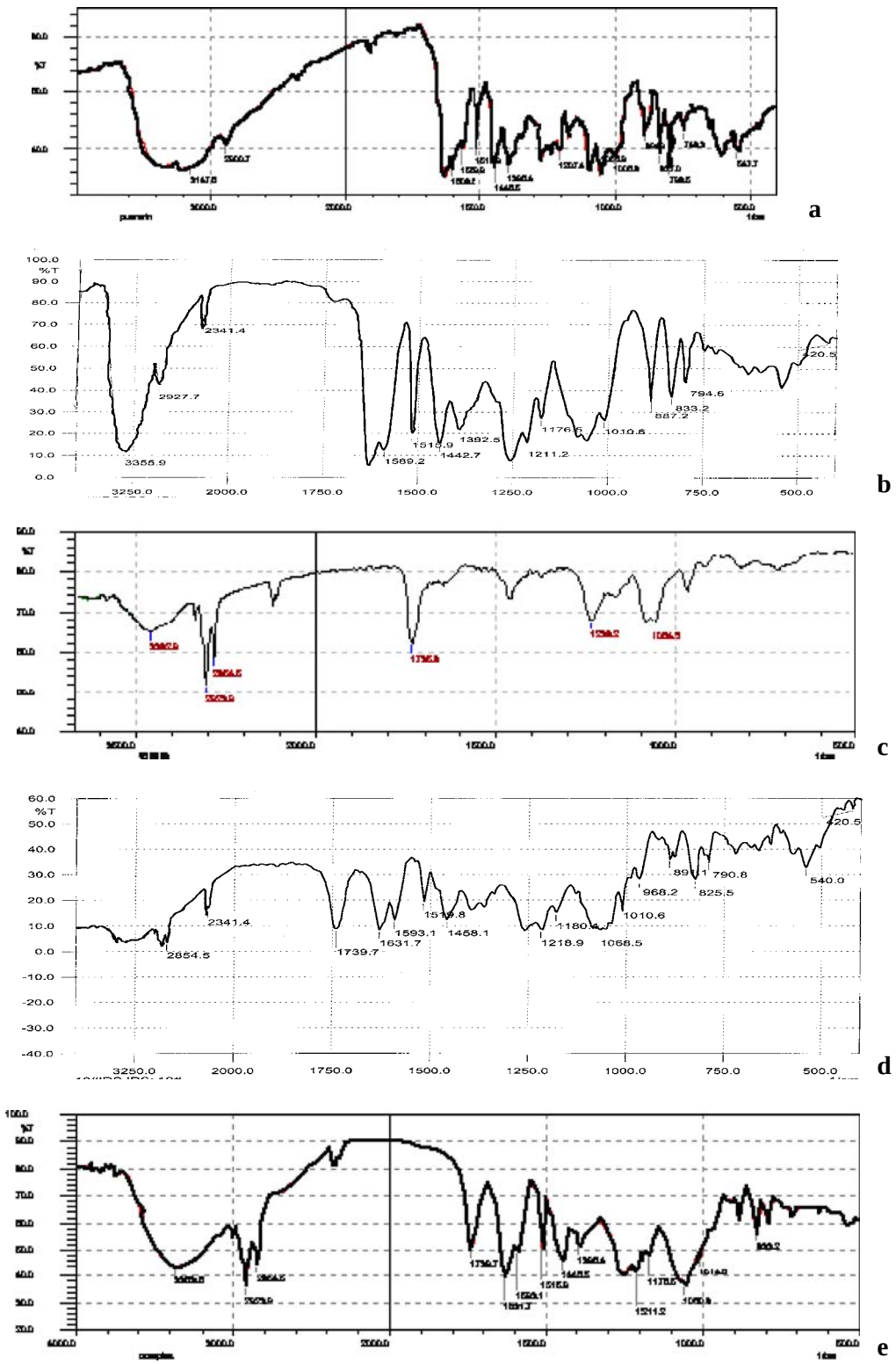

Fig. 8. IR spectra of **a** unprocessed Pur, **b** SEDS–Pur, **c** unprocessed PC, **d** SEDS–PC, **e** SE–PPC, **f** SEDS–PPC, **g** MPPC, **h** FD–PPC, and **i** PM.

of the characteristic Pur bands revealed a modification of its environment, hence providing evidence for the possible interaction occurring between the Pur and carrier. The PPC spectra exhibited a shift in the benzene-ring framework stretching bands from 1608.5 and 1569.9 cm^{-1} to a new band at 1593.1 cm^{-1}, and –C–C vibrations of benzene-ring moved to lower wave number s of 887.2, 833.2 cm^{-1} and 794.6 cm^{-1}, all suggesting a possible change in the environment of benzene-ring framework of Pur.

Spectroscopic changes could also be observed in the polar end of phospholipids where –P=O stretching vibrations changed from 1238.2 cm^{-1} to 1211.2 cm^{-1}. For the non-polar

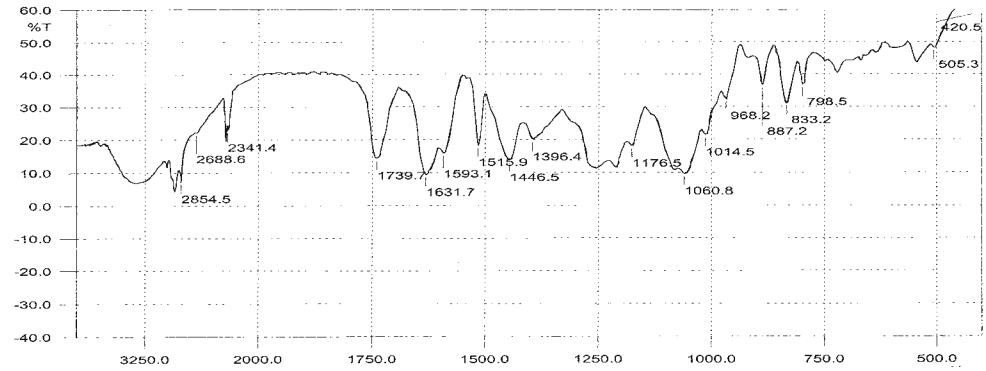

f

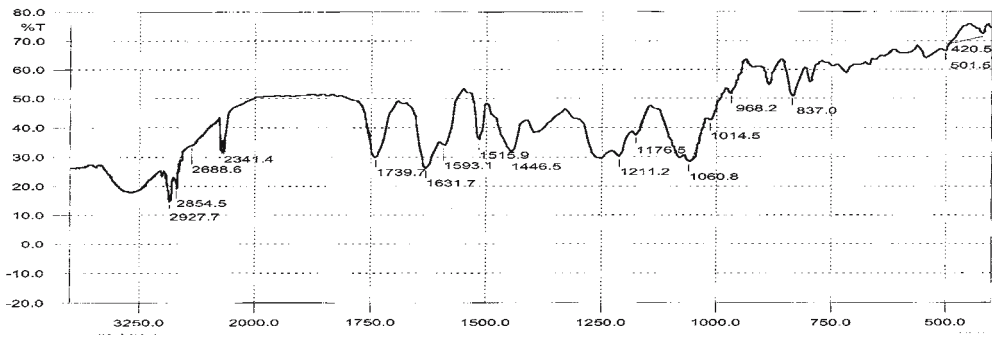

g

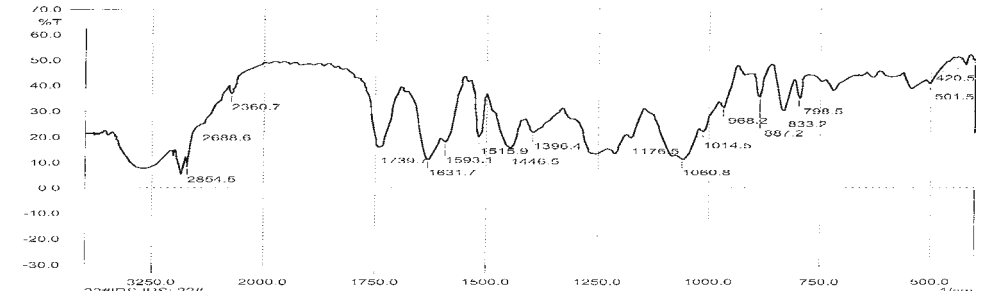

h

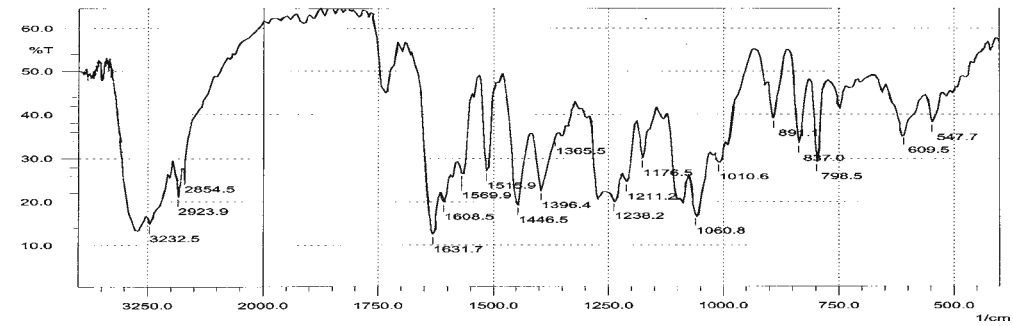

i

Fig. 8. (continued).

Table IV. Wavenumbers in the IR Spectra of PPC and its Components

	Wavenumbers(cm^{-1})								
	Unprocessed Pur	SEDS–Pur	Unprocessed PC	SEDS–PC	SE–PPC	MPPC	FD–PPC	SEDS–PPC	PM
ν_{OH}	3,147.6	3,355.9	3,382.9		3,363.6				3,232.5
									3,382.9
ν_{CH}	2,900.7	2,927.7	2,923.9	2,923.9	2,923.9	2,854.5	2,927.7	2,854.5	2,923.9
			2,854.5	2,854.5	2,854.5		2,854.5		2,854.5
$\nu_{C=O}$	1,631.7		1,735.8	1,739.7	1,739.7	1,739.7	1,739.7	1,739.7	1,735.8
					1,631.7	1,631.7	1,631.7	1,631.7	1,631.7
$\nu_{C=C}$	1,608.5	1,589.2			1,593.1	1,593.1	1,593.1	1,593.1	1,608.5
	1,569.9	1,515.9			1,515.9	1,515.9	1,515.9	1,515.9	1,569.9
	1,515.9	1,442.7			1,446.5	1,446.5	1,446.5	1,446.5	1,515.9
	1,446.5								1,446.5
$\nu_{C-C(benzene)}$	894.9	887.2			887.2	887.2	887.2	887.2	891.1
	837.0	833.2			833.2	833.2	833.2	833.2	837.0
	798.5	794.6			794.6	794.6	798.5	798.5	798.5
$\nu_{P=O}$			1,238.2	1,218.9	1,211.2	1,238.2			1,238.2
ν_{P-O-C}			1,064.6	1,068.5	1,060.8	1,060.8	1,060.8	1,060.8	1,060.8

end of PC, changes were not observed for the –C–H stretching bands of the saturated long fatty acid chain still at 2923.9 and 2854.5 cm^{-1}. To sum up, benzene-ring framework vibration had changed the intensity and had slightly shifted in Pur suggesting complex formation of that part of the molecule with the polar end of PC molecular. These interactions would just result in the decrease of the electron cloud density of the benzene ring in Pur and accordingly the increase of the vibration energy. So the peak at 1569.9 cm^{-1} moved to a higher wave number and appeared as the new peak at 1593.1 cm^{-1} by integrating with the peak at 1608.5 cm^{-1}.

Changes arising from the SEDS process itself were also evaluated by comparing FTIR spectra of SEDS-processed drug, SEDS–PPC with the unprocessed drug, and those of PPC prepared by the other three methods. The results indicated that minor structural changes on a molecular level had occurred due to changes on the physical state of Pur from crystalline into amorphous form though there was no change on its chemical composition. Because amorphous and crystal forms of a drug have nonequivalent spatial relationships that often results in different functional group vibrational modes and different nuclear resonance frequencies. Variations mainly exhibited in the characteristic absorption band of hydroxyl stretching at 3355.9 cm^{-1}, –C–H stretching at 2927.7 cm^{-1} and benzene-ring framework vibrations at 1589.2, 1515.9, 1442.7 cm^{-1} and C–C stretching vibrations at 887.2, 833.2 and 794.6 cm^{-1}. The vibrations at the 1739.7 cm^{-1} of –C=O group, 1218.9 cm^{-1} of –P=O group, and 1068.5 cm^{-1} of –P–O–C in the PC molecular also exhibited a shift after treatment with SEDS compared with raw material. All changes in the spectra of SEDS–Pur and SEDS–PC revealed a modification of the environment of Pur and PC. A possible explanation for this was that all those modifications were induced by SCF processing. The energy provided by SEDS process induced molecular vibration changes. The process employed may influence the properties of the resulting product. The SCF process was considered to be high-energy operation and the energy imputed in SCF process led to the modification of the environment of SEDS–Pur and SEDS–PC. Thus the wave number s shifted to a higher or lower position accordingly. The deep likeness existing among the four spectra of SE–PPC, MPPC, FD–PPC and SEDS–PPC indicated that the different treatment did not induce any perceptible modification of PPC. This result confirmed that the formation mechanism and the interaction position were the same for PPC despite different preparation methods, which was also agreement with the DSC and XRPD results discussed earlier.

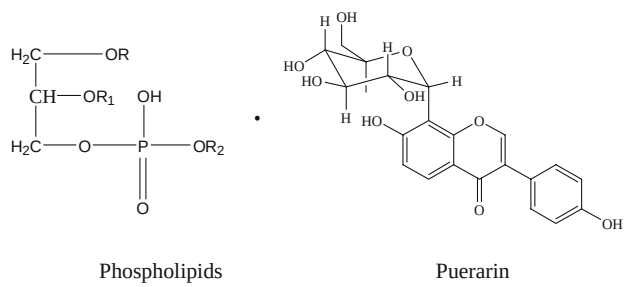

Fig. 9. The structures of phospholipids and puerarin (R and R_1 are the acid radical of cetylic acid, oleic acid, octadcanoic acid or linoleic acid; R_2 is chlorine, amino ethyl alcohol or serine.)

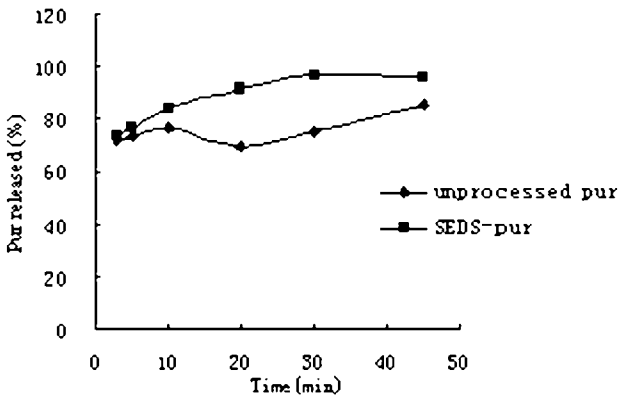

Fig. 10. Dissolution profiles of Pur from unprocessed Pur and SEDS-Pur in artificial gastric juice at 37°C.

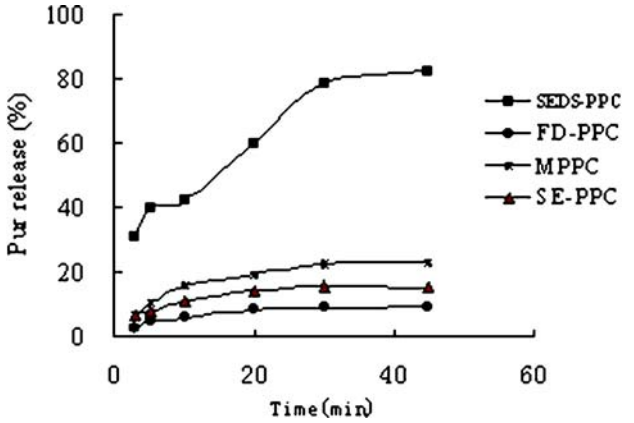

Fig. 11. Dissolution profiles of Pur from PPC prepared by different methods in artificial gastric juice at 37°C.

Solubilities and Dissolution Studies

Solubility studies at the end of 24 h indicated an aqueous solubility of 2.87 mg/ml and 5.49 mg/ml for Pur and SE–PPC, respectively. The solubility of the physical mixture in water was 3.15 mg/ml. SE–PPC significantly increased puerarin solubility by 1.91 fold. The observed puerarin solubility increase by formation of PPC was in close agreement with that reported by Wu *et al*. (54). The increase in solubility of Pur by PPC can be explained by the solubilization resulted from the formation of micelle in the medium and by the amorphous characteristics of the complex though the improvement was not very remarkable. As an amphiphilic surfactant, phospholipids could increase the solubility of the drug by the action of wetting and dispersion. That's why the solubility of the physical mixture was also enhanced. The experimental values of the equilibrium solubility of MPPC, FD–PPC, SEDS–PPC and SEDS–Pur, were 3.98, 3.68, 3.43 and 3.39 mg/ml. Thus the amorphous physical characteristics and the better dispersion into the medium of the SEDS–Pur powder ascribed to the fluffy appearance do appear to affect the drug solubility in water even if no real statistically difference was found between them. It must be emphasized that solid dissolution is a complex operation influenced by a great number of factors, not only the particle size. Differences in crystal habit, surface area, surface energies, particle size and wettability may all play a role in affecting the dissolution rate of powder (55). Though it was determined that the equilibrium solubilities of MPPC, FD–PPC and SEDS–PPC samples were the same as the SEDS–Pur and even smaller than SE–PPC, the samples exhibited different dissolution rates because of differences in their morphology and particle sizes. From the dissolution profiles depicted in Fig. 10, a remarkable increase of the Pur dissolution rate was achieved by its processing with supercritical CO_2 as compared to the raw materials especially after 10 min. This was also the expected result according to the increased solubility and the former discussion on particle morphology and size.

Dissolution profiles of PPC systems prepared by the four processing methods were compared in Fig. 11. It is apparent from Fig. 11 that the initial dissolution rate of SEDS–PPC sample was much higher than the other three conventionally processed PPC samples, although its equilibrium solubility was the same with FD–PPC and MPPC, and even smaller than SE–PPC. A possible explanation for the equivalence of the equilibrium solubility of SEDS processed samples, despite their amorphous state, could be due to recristallization/precipitation from the saturated solution since the amorphous state was usually not stable. The higher dissolution rate of SEDS samples was obviously caused by the increased surface area in the case of much smaller microparticles, as shown in the SEM pictures. As a matter of fact, micronization, whatever the process, may alter the solid morphology to a more or less extent. This is of major importance when the solid exhibits polymorphism and when an amorphous phase is formed, creating unexpected behavior and/or unstable properties (24). So the dissolution of PPC in the amorphous form was originally expected to be faster than the pure drug because of its higher free energy, greater molecular motion and stronger thermodynamic properties compared with the crystal material. But on the contrary, the results from our research showed that the PPC dissolution in artificial gastric solution decreased compared with the pure Pur. PPC powder presented a little more viscous state because of the phospholipids viscosity and this hindered the release of Pur from PPC in the dissolution test. Otherwise according to the Noyes–Whitney equation: dC/dt=DS(Cs–Co)/Vh, where D is the diffusion coefficient, S is the surface area, Cs is saturated concentration in the diffused layer and Co is the drug concentration in medium, the dissolution rate was proportional to D, S, (Cs–Co) and inverse proportional to the diffusion layer thickness of h and medium volume of V. Compared with Pur, h increased and difference between Cs and Co enlarged for PPC systems all leading to the decreased dissolution rate.

It was consistent with what we forecast that compared with other three conventional preparation methods the SEDS technique was helpful to improve the dissolution rate of PPC. Since the SEDS–PPC gained much advantage over the particle size, morphology, and dissolution behavior *in vitro*, the potential for the improvement on the bioavailability by SEDS–PPC was also foreseeable.

CONCLUSION

In this study, GAS had a profound effect on the polymorphism of Pur. Using GAS technique we produced puerarin into another crystal form approved by DSC, XRPD, and IR analysis with more ordered appearance, cleaner surface, directionally arrangement in prisms and smaller size compared with the unprocessed drug. Pur prepared by SEDS was arranged in particles in amorphous state and a homogeneous distribution with enhanced solubility and dissolution rate. Although the solid state analysis using DSC, XRPD and IR of the PPC systems with SEDS, solvent evaporation, freeze-drying and mircronization technologies indicated the same physical state, thermodynamic activities and structure compositions, the PPC prepared by supercritical method exhibited more rapidly dissolution among four samples. In addition, supercritical fluid technology for the preparation of puerarin phospholipids complex has been proven to have significant advantages over particle size and morphology.

The results of this study demonstrated that a supercritical process could be an efficient method for pharmaceutical compounds recrystallization or phospholipids complex formation with the improved physicochemical properties. Further investigation should be conducted regarding the *in vivo* performance of SEDS processed PPC to support our *in vitro* findings.

REFERENCES

1. L. P. Ruan, S. Chen, B. Y. Yu, D. N. Zhu, G. A. Cordell, and S. X. Qiu. Prediction of human absorption of natural compounds by the non-everted rat intestinal sac model. *Eur. J. Med. Chem.* **41**:605–610 (2006).
2. J. Wang, M. Ji, W. Y. Hua, and D. Z. Dai. Development of puerarin. *Prog. Pharm. Sci.* **27**:70–73 (2003).
3. Q. L. Zhu and X. R. Lv. The pharmacology and clinical application of Puerarin. *Chin. Trad. Herb. Drugs.* **28**:693–696 (1997).
4. F. Lili, D. O. Keefe, and W. J. Powell Jr. The effect of Puerarin on the regional coronary blood flow and heart arterial blood flow dynamics of the acute myocardial ischemia dogs. *Acta. Pharm. Sin.* **19**:801–807 (1984).
5. Z. H. Wu, Y. Q. Zu, H. Y. Yan, and G. Chen. The study on the solubility of Puerarin and the solubilizing effect of macromolecule polymers on it. *Chin. Trad. Herb. Drugs* **30**:88–89 (1999).
6. J. P. Guo and T. Y. Zhao. The study on the *in vitro* dissolution of Pueraria flavones dripping pill. *Chin. Trad. Herb. Drugs* **26**: 298–299 (1995).
7. X. L. Jin and X. Y. Zhu. Pharmacokinetics of puerarin in rats, rabbits and dogs. *Acta. Pharm. Sin.* **13**:284–288 (1992).
8. X. L. Jin, G. F. Chen, and X. Y. Zhu. Pharmacokinetics of puerarin in healthy volunteers. *Chin. J. Clin. Pharmacol.* **7**:115–118 (1991).
9. M. Lu, N. Li, D. P. Meng, Y. R. Guo, and Y. H. Chen. Study on the pharmacokinetics of puerarin in patients with diabetic nephropathy. *Chin. J. Hosp. Pharm.* **20**:18–720 (2000).
10. J. K. Prasain, K. Jones, N. Brissie, R. Moore, J. M. Wyss, and S. Barnes. Identification of puerarin and its metabolites in rats by liquid chromatography-tandem mass spectrometry. *J. Agric. Food. Chem.* **52**:3708–3712 (2004).
11. A. L. Simons, M. Renouf, S. Hendrich, and P. A. Murphy. Human gut microbial degradation of flavonoids: Structure–function relationship. *J. Agric. Food Chem.* **53**:4258–4263 (2005).
12. D. J. Zhou, H. Y. Zhao, and Y. L. Yang. The absorption of puerarin in rats' intestines. *J. of Beijing Univ. of Chem. Tech.* **33**:106–108 (2006).
13. D. O. Thompson. Cyclodextrins-enabling excipients: their present and future use in pharmaceuticals. *Crit. Rev. Ther. Drug Carrier Syst.* **14**:104–106 (1997).
14. M. Bialecka. The Effect of bioflavonoids and lecithin on the course of experimental atherosclerosis in rabbits. *Annu. Acad. Med. Stein.* **43**:41–43 (1997).
15. N. I. Payne, R. F. Cosgrove, A. P. Green, and L. Liu. *In vivo* studies of amphotericin B liposomes derived from proliposomes: effect of formulation on toxicity and tissue disposition of the drug in mice. *J. Pharm. Pharmacol.* **39**:24–28 (1987).
16. S. Kimura. Solubilization of dolichol with lipids. JP. Patent No. 61,194,024 (1986).
17. E. Bombardelli, G. Patri, and R. Pozzi. Complexes of saponins and their aglycons with phospholipids and pharmaceutical and cosmetic compositions containing them. US Patent No. 5, 166,139 (1992).
18. Y. N. Jiang, H. Y. Mo, and J. M. Chen. Study on pharmacokinetic of herba epimeddi total flavonoids and their phytosomes in rats. *Chin. J. Hosp. Pharm.* **22**:582–585 (2002).
19. J. M. Wu, D. W. Chen, and R. H. Zhang. Study on the bioavailability of PPC by using HPLC. *Biomed. Chromatogr.* **13**:493–495 (1999).
20. T. Khazaeinia and F. Jamili. A comparision of gastrointestinal permeability induced by diclofenac–phospholipid complex with diclofenac acid and its sodium salt. *J. Pharm. Pharm. Sci.* **6**:351–358 (2003).
21. S. A. Elkheshen, O. A. Sammour, M. H. A1-Shaboury, and B. T. A1-Quadeib. Enhancement of dissolution and bioavailability of piroxicam via solid dispersion with phospholipid. *B. Faculty Pharm.* **39**:309–320 (2001).
22. Y. Li, W. S. Pan, S. L. Chen, H. X. Xu, D. J. Yang, and S. C. Chan. Pharmacokinetic, tissue distribution, and excretion of puerarin and puerarin–phospholipid complex in rats. *Drug. Dev. Ind. Pharm.* **32**:413–422 (2006).
23. Y. Li, W. S. Pan, S. L. Chen, D. J. Yang, S. C. Chan, and H. X. Xu. Studies on preparation of puerarin phytosomes and their solid dispersions. *Chin. Pharm. J.* **37**:695–697 (2006).
24. M. Perrut, J. Jung, and F. Leboeuf. Enhancement of dissolution rate of poly-soluble active ingredients by supercritical fluid processes. Part I: Micronization of neat particles. *Int. J. Pharm.* **288**:3–10 (2005).
25. E. Reverchon, G. Della Porta, and M. G. Failivene. Progress parameters and morphology in amoxicillin micro and submicro particles generation by supercritical antisolvent precipitation. *J. Supercrit. Fluids.* **17**:239–248 (2000).
26. B. Warwick, F. Dehghani, N. R. Foster, J. R. Biffin, and H. L. Regtop. Synthesis, purification, and micronization of pharmaceuticals using the gas antisolvent technique. *Ind. Eng. Chem. Res.* **39**:4571–4573 (2000).
27. M. Moneghini, I. Kikic, D. Voinovich, B. Perissutti, P. Alessi, A. Cortesi, F. Princivalle, and D. Solinas. Study of solid state of carbamazepine after processing with gas anti-solvent technique. *Eur. J. Pharm. Biopharm.* **56**:281–289 (2003).
28. E. Badens, C. Magnan, and G. Charbit. Microparticles of soy lecithin formed by supercritical process. *Biotechnol. Bioeng.* **72**:194–204 (2001).
29. E. Rodier, H. Lochard, M. Sauceau, J. Letourneau, B. Freiss, and J. Fages. A three step supercritical process to improve the dissolution rate of Eflucimibe. *Eur. J. Pharm. Sci.* **26**:184–193 (2005).
30. S. Sethia and E. Squillante. Physicochemical characterization of solid dispersion of carbamazepine formulated by supercritical carbon dioxide and conventional solvent evaporation method. *J. Pharm. Sci.* **91**:1948–1957 (2002).
31. N. Elvassore, A. Bertucco, and P. Caliceti. Production of insulin-loaded poly(ethylene glycol)/poly(l-lactide)(PEG/PLA) nanoparticles by gas antisolvent techniques. *J. Pharm. Sci.* **90**:1628–1636 (2001).
32. R. Ghaderi, P. Artursson, and J. Carlfors. Preparation of biodegradable microparticles using solution-enhanced dispersion by supercritical fluids (SEDS). *Pharm. Res.* **16**:676–681 (1999).
33. A. R. C. Duarte, M. S. Costa, A. L. Simplicio, M. M. Cardoso, and C. M. M. Duart. Preparation of controlled release microspheres using supercritical fluid technology for delivery of anti-inflammatory drugs. *Int. J. Pharm.* **308**:168–174 (2006).
34. E. Reverchon and I. D. Marco. Supercritical antisolvent micronization of Cefonicid: thermodynamic interpretation of results. *J. Supercrit. Fluids.* **31**:207–215 (2004).
35. W. K. Snavely, B. Subramaniam, R. A. Rajewski, and M. R. Defelippis. Micronization of insulin from halogenated alcohol solution using supercritical carbon dioxide as an antisolvent. *J. Pharm. Sci.* **91**:2026–2038 (2002).
36. O. I. Corrigan and A. M. Crean. Comparative physicochemical properties of hydrocortisone-PVP composites prepared using supercritical carbon dioxide by the GAS anti-solvent recrystallization process, by coprecipitation and by spray drying. *Int. J. Pharm.* **245**:75–82 (2002).
37. P. Pathak, M. J. Meziani, T. Desai, and Y. P. Sun. Nanosizing drug particles in supercritical fluid processing. *J. Am. Chem. Soc.* **126**:10842–10843 (2004).
38. M. J. Meziani, P. Pathak, R. Hurezeanu, M. C. Thies, R. M. Enick, and Y. P. Sun. Supercritical-fluid processing technique for nanoscale polymer particles. *Angew. Chem. Int. Ed.* **43**:704–707 (2004).
39. J. H. Kim, T. E. Paxton, and D. L. Tomasko. Microencapsulation of naproxen using rapid expansion of supercritical solutions. *Biotechnol. Prog.* **12**:650–661 (1996).
40. Y. L. Wang, D. G. Wei, R. Dave, R. Pfeffer, M. Sauceau, J. J. Letourneau, and J. Fages. Extraction and precipitation particles coating using supercritical CO_2. *Powder. Technol.* **127**:32–44 (2002).
41. K. X. Chen, X. Y. Zhang, J. Pan, and W. H. Yin. Recrystallization of andrographolide using the supercritical fluid antisolvent process. *J. Cryst. Growth.* **274**:226–232 (2005).

42. C. Magnan, E. Badens, N. Commenges, and G. Charbit. Soy lecithin micronization by precipitation with a compressed fluid antisolvent-influence of process parameters. *J. Supercrit. Fluids.* **19**:69–77 (2000).
43. S. Bristow, T. Shekunov, B. Y. Shekunov, and P. York. Analysis of the supersaturation and precipitation process with supercritical CO_2. *J. Supercrit. Fluids.* **21**:257–271 (2001).
44. M. Rehman, B. Y. Shekunov, P. York, and P. Colthorpe. Solubility and precipitation of nicotinic acid in supercritical carbon dioxide. *J. Pharm. Sci.* **90**:1570–1582 (2001).
45. J. Fages, H. Lochard, J. J. Letourneau, M. Sauceau, and E. Rodier. Particle generation for pharmaceutical applications using supercritical fluid technology. *Powder. Technol.* **141**:219–226 (2004).
46. D. Y. Sang, M. S. Kim, and J. C. Lee. Recrystallization of sulfathiazole and chlorpropamide using the supercritical fluid antisolvent process. *J. Supercrit. Fluids.* **25**:143–154 (2003).
47. M. Charoenchaitrakool, F. Dehghani, and N. R. Foster. Utilization of supercritical carbon dioxide for complex formation of ibuprofen and methyl-β-cyclodextrin. *Int. J. Pharm.* **239**:103–112 (2002).
48. T. M. Martin, N. Bandi, R. Shulz, C. B. Roberts, and U. B. Kompella. Preparation of budesonide and budesonide-PLA microparticles using supercritical fluid precipitation technology. *AAPS. PharmSciTech* **3**:1–11 (2002).
49. G. X. Zhai. The research on puerarin phospholipids solid dispersion. Shenyang Pharmaceutical University Thesis. 37–38.
50. W. Li, Y. Y. Shao, G. D. Huang, and L. X. Hu. The purifying and TG–DTA–DTG thermal analysis of the lecithin. *Sci. Tech. Food. Ind.* **22**:9–11 (2001).
51. S. Sethia and E. Squillante. Solid dispersion of carbamazepine in PVP K30 by conventional solvent evaporation and supercritical methods. *Int. J. Pharm.* **272**:1–10 (2004).
52. Q. H. Wang, Y. Y. Feng, S. L. Yang, and L. F. Chen. Study on the phospha-tidycholine by means of infrared and ultraviolet spectroscopy. *J. Nanjing Normal Univ. (Nat. Sci. Ed.)* **17**:51–53 (1994).
53. Y. Han, Y. Zhou, and Y. F. Zhao. The purification and the identification of lecithin and its application. *Amino Acids Biotic. Res.* **23**:28–31 (2001).
54. J. M. Wu and D. W. Chen. Study on the physico-chemical properties of baicalin-phospholipid complex. *Chin. Pharm. J.* **36**:173–177 (2001).
55. D. J. Jarmer, C. S. Lengsfeld, K. S. Anseth, and T. W. Randolph. Supercritical fluid crystallization of griseofulvin: Crystal habit modification with a selective growth inhibitor. *J. Pharm. Sci.* **94**:2688–2702 (2005).